Fracture surface investigations of API pipes welded with parameters determined by Taguchi method

Elif Asikuzun[*1], Cemil Cetinkaya[2], Mustafa Boz[3], Hakan Ada[4]

Abstract

In this study, SEM images of the samples taken from welded nick break tests of API 5L X65 pipe joints, whose welding parameters were determined by Taguchi method, were examined. As a result of the investigations, the elongations and orientations exhibited by the grains showed that ductile and brittle fractures were observed in the welded joints. As it was observed from equiaxed, honeycomb like images that the fractures exhibited a ductile behavior. Brittle fractures that occurred due to cleavage breaks in some regions were detected. An apparent effect of welding direction was observed in fracture behavior. It was detected from the SEM images that a ductile fracture structure had occurred in all joints that were performed from bottom to top, while it was observed in the joints performed from top to bottom that generally cleavage planes had developed along with fibrous structures in places, therefore brittle fractures had occurred.

Keywords: API 5L X65, fracture surface, SEM, Taguchi method

1. INTRODUCTION

Petroleum and natural gas have an important place in human life and international relations as the most important energy sources. Recent history has revealed that oil and natural gas are not only important energy resources, but also have political, economic, cultural and military dimensions and thus have strategic importance [1]. Transportation of oil and natural gas, which have such an economic and strategic importance, from their sources to separation stations and of end products obtained in the separation process to the places of use is an extremely important operation. This transportation operation carried out at high pressures is performed only with large diameter steel pipes [2]. It is well known that the easiest and cheapest way to transport oil and gas products to far destinations is to use pipelines. Piping systems with modern designs all over the world transport goods, petroleum, petroleum products and natural gas from production sites to consumers. Increasing demand for energy in the world also requires construction of high-pressure pipelines with high transport capacity [3].

Today, steels used in the manufacture of natural gas and petroleum line pipes are produced according to the API (American Petroleum Institute) 5L standard. API 5L X65 steel is a type of high-strength and low alloy steel preferred in construction works of pipelines [4]. In API 5L standard, the main feature of "X" class materials is that fine-grained ferrite and perlite structures are obtained as a result of thermomechanical processes. These materials, that are frequently used especially in high pressure pipelines, are produced with controlled thermomechanical rolling method, in which fine-grained acicular ferrites are intensely present [5-7]. The numbers on the sides of X series steel indicate the pressure corresponding to yield strength of the material. For

---

* Corresponding Author
[1] Kastamonu University, easikuzun@kastamonu.edu.tr
[2] Gazi University, ccetin@gazi.edu.tr
[3] Karabük University, mboz@karabuk.edu.tr
[4] Kastamonu University, hakanada@kastamonu.edu.tr

example, the expression X65 states that the material is an X series steel, while it has a yield strength corresponding to a minimum pressure of 65 kpsi (65.000 psi). The main microalloy element in API steels is Niobium in combination with titanium and vanadium (Nb/V, Nb/Ti, Nb/V/Ti). These combinations affect yield stress and toughness of the steel positively [8-10]. These steels are widely used in oil and gas transportation via pipelines due to their low cost, easy availability and high resistance properties [3, 11, 12].

In this study, SEM images of the samples taken from welded nick break tests of API 5L X65 pipe joints, whose welding parameters were determined by Taguchi method, were examined. Welded joint process of the pipes were performed at Gazi University Technical Sciences Vocational School, nick break tests were conducted at Emek Pipe Machine Industry and Trade Inc. Ankara Facility, and SEM investigations of the fracture surfaces were performed at Kastamonu University Central Research Laboratory.

2. EXPERIMENTAL STUDIES

This study was carried out in two stages. In the first stage, welding of pipes was performed and in the second stage, SEM images obtained from fracture surfaces of the welded joints were evaluated. Using Taguchi method during the welding process, which is the first stage, it was aimed to produce real and rational solutions to contribute to industrial applications by determining the optimal factors (variables). In the second stage, analyzing fracture structure of the joints which were welded according to the parameters determined by Taguchi method, it was aimed to determine fracture behaviors of the welded joints when they were subjected to mechanical loads.

For this purpose, electric arc welding method with covered electrode, widely used in welded joint process of pipes in natural gas and oil pipelines, was preferred. In welding operations, variables such as strength of current value, electrode type (Cellulosic or Basic) and welding direction (top to bottom or bottom to top) were taken as input parameters. In the experiments, the strength of current values used for welded joints were 110-140, 120-150, 130-160, 140-170, 150-180, 160-190, 170-200 and 180-210 A.

After specifying factors and levels, welded joint operations were carried out with Taguchi L16 experimental setup (8*2*2). The factors and levels determined by Taguchi method are given in Table 1, and Taguchi L16 experimental setup is given in Table 2.

Table 1. Experiment factors and levels

| | Experiment Factors | Experiment Levels | | | | | | | |
		1	2	3	4	5	6	7	8
A	Strength of Current (A)	110–140	120–150	130-160	140-170	150-180	160-190	170–200	180–210
B	Welding Direction	Bottom to Top ↑	Top to Bottom ↓						
C	Electrode Type	Cellulosic	Basic						

Table 2. Taguchi L_{16} experimental setup

Experiment No	-A- (Strength of Current) (Amper)	-B- (Welding Direction)	-C- (Electrode Type)
1	1 (110 – 140)	1 (Bottom to top ↑)	1 (Cellulosic)
2	1 (110 – 140)	2 (Top to bottom ↓)	2 (Basic)
3	2 (120 – 150)	1 (Bottom to top ↑)	1 (Cellulosic)
4	2 (120 – 150)	2 (Top to bottom ↓)	2 (Basic)
5	3 (130 – 160)	1 (Bottom to top ↑)	1 (Cellulosic)
6	3 (130 – 160)	2 (Top to bottom ↓)	2 (Basic)
7	4 (140 – 170)	1 (Bottom to top ↑)	1 (Cellulosic)
8	4 (140 – 170)	2 (Top to bottom ↓)	2 (Basic)
9	5 (150 – 180)	1 (Bottom to top ↑)	2 (Basic)
10	5 (150 – 180)	2 (Top to bottom ↓)	1 (Cellulosic)
11	6 (160 – 190)	1 (Bottom to top ↑)	2 (Basic)
12	6 (160 – 190)	2 (Top to bottom ↓)	1 (Cellulosic)
13	7 (170 – 200)	1 (Bottom to top ↑)	2 (Basic)
14	7 (170 – 200)	2 (Top to bottom ↓)	1 (Cellulosic)
15	8 (180 – 210)	1 (Bottom to top ↑)	2 (Basic)
16	8 (180 – 210)	2 (Top to bottom ↓)	1 (Cellulosic)

3. MATERIAL AND METHOD

In the experiments, steel pipes of API 5L X65 quality with 1066.8 mm (42") diameter and 12.7 mm cross section thickness, whose chemical composition and mechanical properties are given in Table 3, were used. Cellulosic and basic electrodeswere used as additional materials. In joints made with cellulosic electrode, AWS E6010 electrode (Table 4) with a diameter of 3.25 mm was used in root pass, while AWS E8010 electrode (Table 5) with a diameter of 4.00 mm was used in hot pass, intermediate pass and cap pass. In joints made with basic electrodes, AWS E9018-D1-H4 electrodes (Table 6) was used; an electrode with a diameter of 3.25 mm was preferred in root pass and an electrode with a diameter of 4.00 mm was preferred in other passes. Steel pipes prepared for welding procedure were cut to 300 mm width by an automatic plasma cutting machine. A 30° V welding groove was opened in the cut pipes. The welding groove geometry and pass sequence of the welded joint process are given in Figure 1.

Table 3. Chemical composition and mechanical properties of X65 material used in the experiments

	C	Si	Mn	P	S	Cr	Ni	Mo
Element (%)	0.064	0.29	1.61	0.008	0.0018	0.021	0.001	0.001
	Cu	Al	Ti	V	Nb	N	Fe	C_{Es}
	0.008	0.035	0.023	0.051	0.052	0.028	97.83	0.348

Mechanical Properties	Yield Strength (MPa)	Tensile Strength (MPa)	Elongation (%) (min.)	Impact Energy (0°C) (Joule)
	566	650	34	209

Table 4. Chemical analysis and mechanical properties of AWS/ASME FA.5.1. E6010 cellulosic electrode

Typical Chemical Analysis of Weld Metal			Typical Mechanical Properties of Weld Metal (%)			
C	Si	Mn	Yield Str. (min) (N/mm2)	Tensile Str. (min) (N/mm2)	Elongation (%)	Notch Impact Energy (0 °C) (min) (Joule)
0.10	0.20	0.50	470	530	26	60

Table 5. Chemical analysis and mechanical properties of AWS/ASME FA.5.1. E8010 cellulosic electrode

Typical Chemical Analysis of Weld Metal				Typical Mechanical Properties of Weld Metal (%)			
C	Si	Mn	Ni	Yield Str. (min) (N/mm^2)	Tensile Str. (min) (N/mm^2)	Elongation (%)	Notch Impact Energy (-20 °C) (min) (Joule)
0.10	0.20	0.80	0.90	500	570	24	60

Table 6. Chemical analysis and mechanical properties of AWS A5.5. E9018-D1-H4 basic electrode

Typical Chemical Analysis of Weld Metal				Typical Mechanical Properties of Weld Metal (%)		
C	Si	Mn	Mo	Yield Str. (min) (N/mm2)	Tensile Str. (N/mm2)	Notch Impact Energy (-50 °C) (min) (Joule)
0.075	0.40	1.60	0.45	550	610-780	47

Technical specifications of the rectifier type welding machine used in welded joints are shown in Table 7.
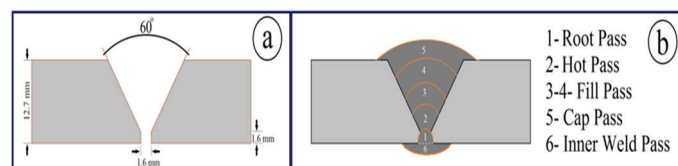
Figure 1. a) Welding groove geometry, b) Pass sequence

Table 7. Technical specifications of the rectifier type welding machine used in welded joints

Mains Voltage (3 Phase) (V)	380 / 50 Hz
Power From Mains (kVA)	20 (%35)
Current From Mains (A)	31 (%35)
Recommended Mains Safety Fuse (A)	3 x 32
Welding Current Regulation Range (ADC)	60 – 350
Rated Welding Current (ADC)	350 (%35)
Open Circuit Voltage (VDC)	54 – 64
Electrode Diameter (mm)	2.00 – 5.00
Dimensions (u x g x y) (mm)	950x660x 650
Weight (kg)	125
Protection Class	IP 22

Figure 2. Schematic image of welding operation

As seen in Figure 2, each experiment was subjected to welding operations from top to bottom and bottom to top so that half pipes were joined. The pipe material prepared for welding operation is given in Figure 3.

Figure 3. Pipes prepared for welding operation

Considering the fusion strength and metal stacking capacity of the electrode and the need to increase strength of current values during passes in welding operations, the Taguchi L16 (8*2*2) experimental setup given in Table 2 was rearranged as specified in Table 8. In the experiments, the root passes were welded at a constant current (100 Amperes) and strength of current value was increased by 10 Amperes at each pass in hot passes. In order to eliminate any possible errors that might occur in the root pass, the strength of current in the cap pass (5th pass) was also used for welding in the 6th pass (Figure 1-b). In welded joints, the welding speed was kept constant and welding was carried out at a welding speed of 120 mm/min in the root pass and 150 mm/min in other passes. The basic electrodes employed in the experiments were dried at 250 - 300 ºC for 1 hour and used in welding operations without any delay, while the cellulosic electrodes were used without drying due to their feature.

Table 8. Parameters generated by Taguchi L_{16} experimental setup and used in the experiments

Experiment No	Welding Direction	Electrode Type	Strength of current (Ampere)					
			Root Pass	Hot Pas	Fill Pass	Cap Pass	Inner Pass	
			Ø 3,25 mm			Ø 4,0 mm		
			-Pass 1-	-Pass 2-	-Pass3-	-Pass 4-	-Pass 5-	-Pass 6-
1	Bottom to Top ↑	Cellulosic	100	110	120	130	140	140
2	Top to Bottom ↓	Basic						
3	Bottom to Top ↑	Cellulosic	100	120	130	140	150	150
4	Top to Bottom ↓	Basic						
5	Bottom to Top ↑	Cellulosic	100	130	140	150	160	160
6	Top to Bottom ↓	Basic						
7	Bottom to Top ↑	Cellulosic	100	140	150	160	170	170
8	Top to Bottom ↓	Basic						
9	Bottom to Top ↑	Basic	100	150	160	170	180	180
10	Top to Bottom ↓	Cellulosic						
11	Bottom to Top ↑	Basic	100	160	170	180	190	190
12	Top to Bottom ↓	Cellulosic						
13	Bottom to Top ↑	Basic	100	170	180	190	200	200
14	Top to Bottom ↓	Cellulosic						
15	Bottom to Top ↑	Basic	100	180	190	200	210	210
16	Top to Bottom ↓	Cellulosic						

Welded joints were carried out in accordance with the parameters given in Table 8 and completed welded pipe joints are shown in Figure 4.

Figure 4. Completed welding operations

Nick Break Tests
Nick break tests were performed to visually examine defects such as inadequate fusion, porosity, slag remnants, etc. in the weld metal and periphery of the materials and to determine fracture behavior under mechanical loads which could cause fracture of welded joints. For this purpose, nick break test samples were taken from 16 welded materials in accordance with API 1104 standard. A schematic view of the nick break test samples and photographs of the samples taken according to these criteria are shown in Figures 5 and 6, respectively.
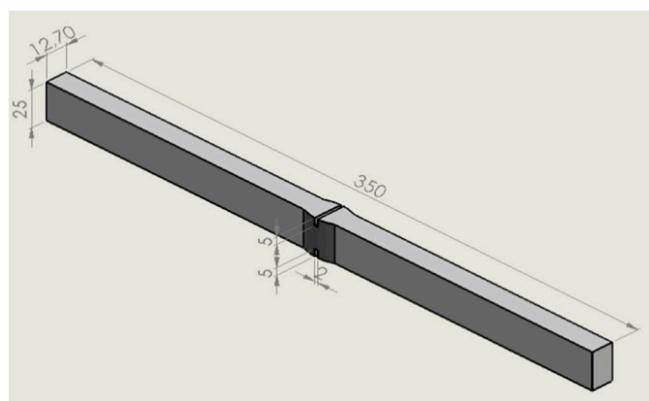
Figure 5. Schematic view of a nick break test sample
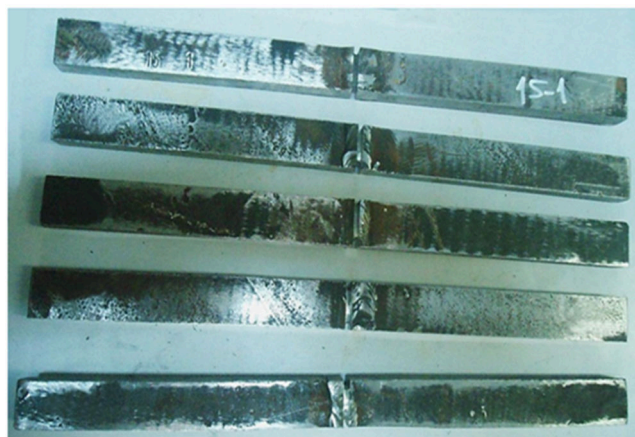
Figure 6. Nick break test samples

4. RESULTS AND DISCUSSION

The results of the nick break test samples prepared in accordance with API 1104 standard are given in Table 9. As a result of nick break tests, the fracture surfaces of the samples were examined first by naked eye and then by taking SEM images from the fractured surfaces.

When the results of the nick break tests given in Table 9 were examined within the scope of visual inspection, welded joints in Experiments 2 and 4 were not accepted due to Lack of fusion or inadequate penetration, but all other welded joint results were regarded acceptable. This suggests that the strength of current applied in Experiments 2 and 4 where welding was performed in bottom to top direction was inadequate. The results obtained from radiographic and macrographic (Figure 7-8) examinations carried out in parallel to our study further support this argument.
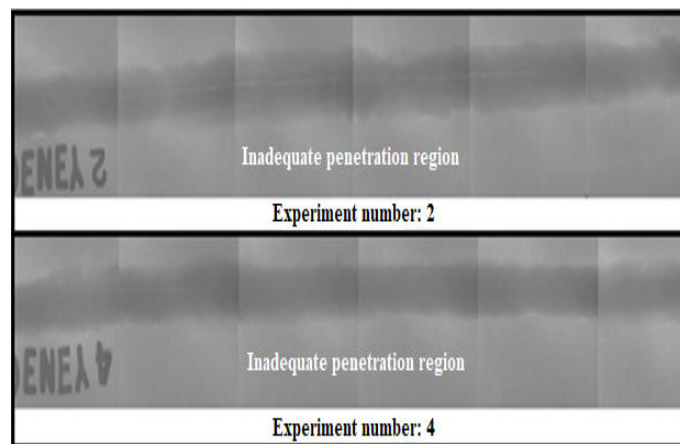
Figure 7. Radiography views
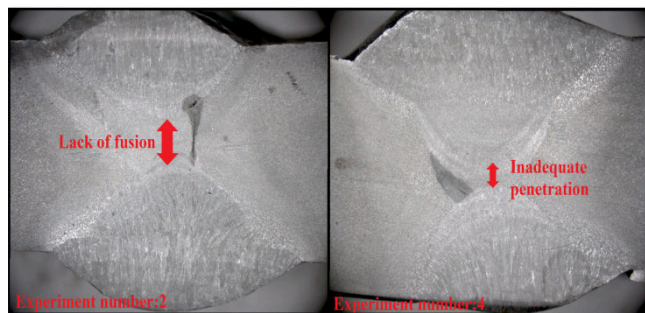
Figure 8. Macrographic images (Experiments 2 and 4)

When radiographic images of Experiments 2 and 4, given in Fig. 7, where welding was performed in downward direction and macrostructure images, given in Fig. 8 were examined. Lack of fusion defects due to insufficient penetration were seen. At this point, the results obtained within the scope of nick break tests were also confirmed by radiographic and macrographic analyses.

Fracture behavior of welded samples was tried to be determined from the SEM images of the fractured surfaces of nick break test samples. Images of the fracture surfaces are given in Figures 9 - 24.
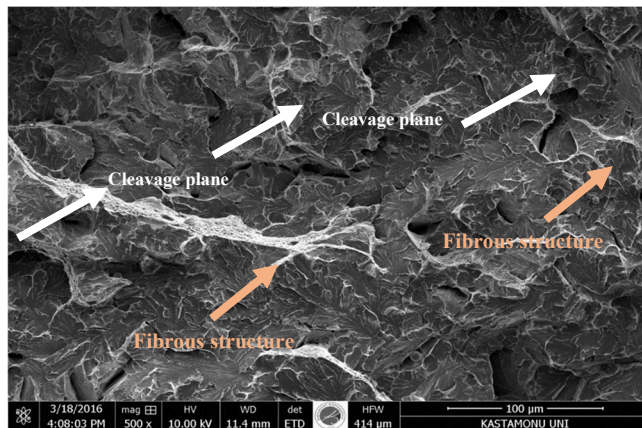
Figure 9. Fracture surface image of Experiment 1
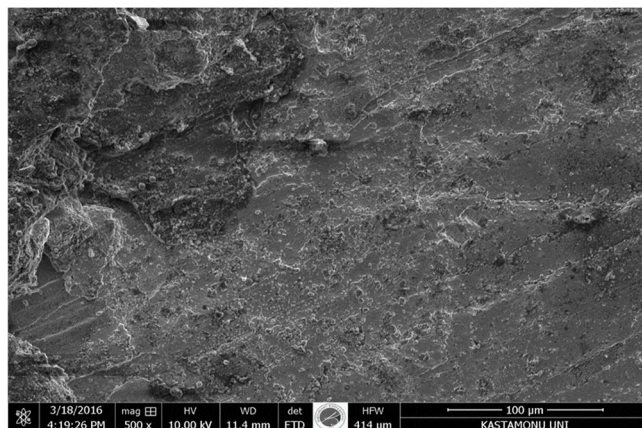
Figure 10. Fracture surface image of Experiment 2

Table 9. Nick break test results

Experiment No	Welding Direction / Electrode / Strength of current Values	Result	Experiment No	Welding Direction / Electrode / Strength of current Values	Result
1	Bottom to Top ↑ / Cellulosic / 110 – 140 A	Accepted	9	Bottom to Top ↑ / Basic / 150 – 180 A	Accepted
2	Top to Bottom ↓ / Basic / 110 – 140 A	Rejected (Lack of fusion)	10	Top to Bottom ↓ / Cellulosic / 150 – 180 A	Accepted
3	Bottom to Top ↑ / Cellulosic / 120 – 150 A	Accepted	11	Bottom to Top ↑ / Basic / 160 – 190 A	Accepted
4	Top to Bottom ↓ / Basic / 120 – 150 A	Rejected (Lack of fusion)	12	Top to Bottom ↓ / Cellulosic / 160 – 190 A	Accepted
5	Bottom to Top ↑ / Cellulosic / 130 – 160 A	Accepted	13	Bottom to Top ↑ / Basic / 170 – 200 A	Accepted
6	Top to Bottom ↓ / Basic / 130 – 160 A	Accepted	14	Top to Bottom ↓ / Cellulosic / 170 – 200 A	Accepted
7	Bottom to Top ↑ / Cellulosic / 140 – 170 A	Accepted	15	Bottom to Top ↑ / Basic / 180 – 210 A	Accepted
8	Top to Bottom ↓ / Basic / 140 – 170 A	Accepted	16	Top to Bottom ↓ / Cellulosic / 180 – 210 A	Accepted
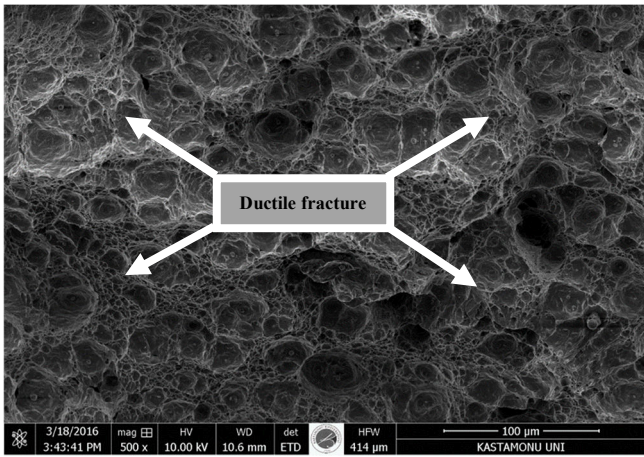
Figure 11. Fracture surface image of Experiment 3
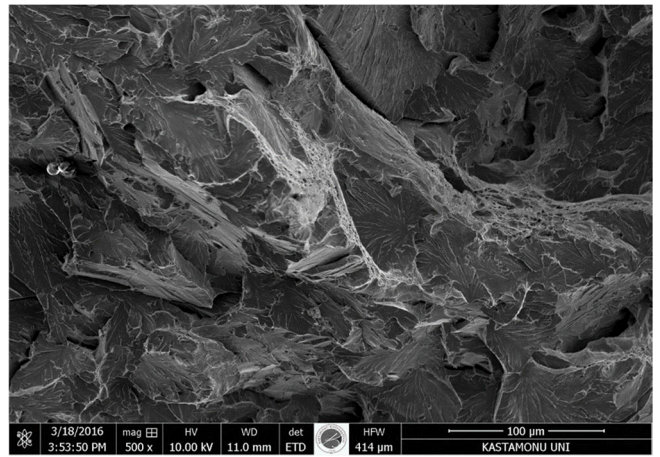
Figure 12. Fracture surface image of Experiment 4
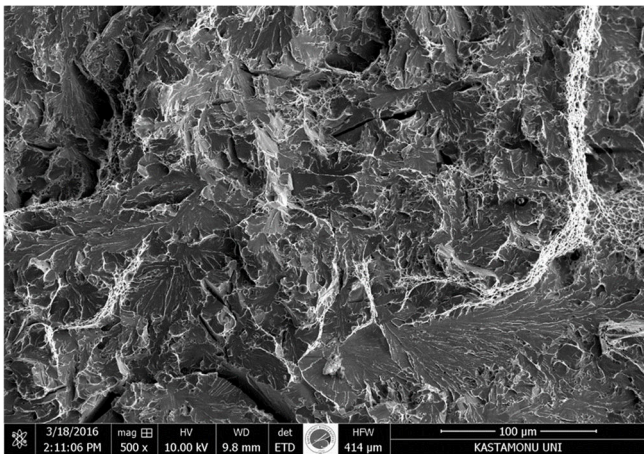
Figure 13. Fracture surface image of Experiment 5
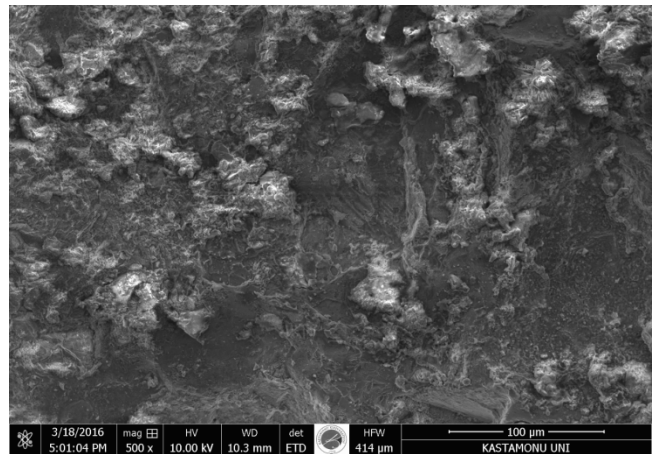
Figure 16. Fracture surface image of Experiment 8
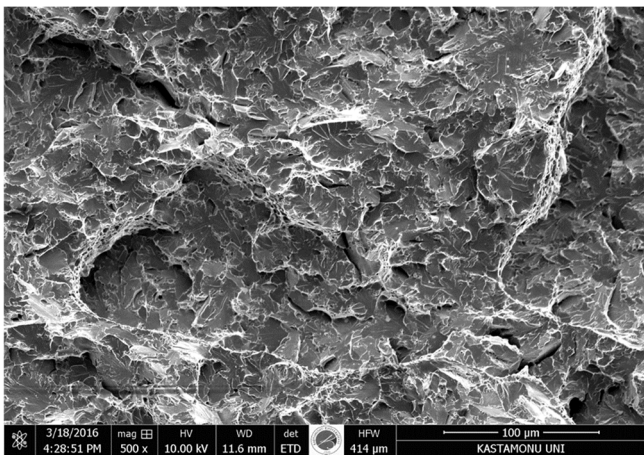
Figure 14. Fracture surface image of Experiment 6
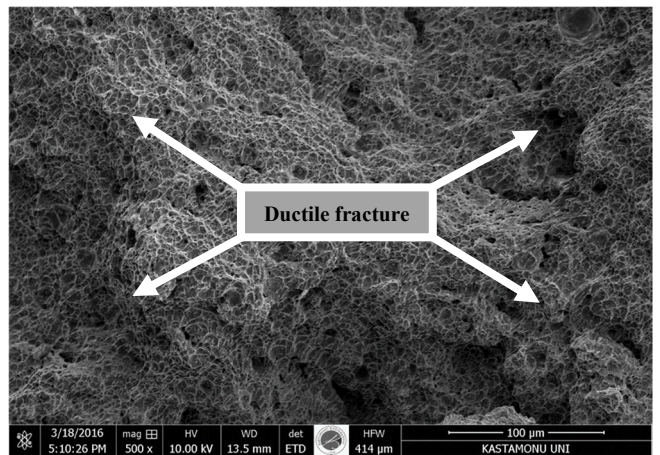
Figure 17. Fracture surface image of Experiment 9
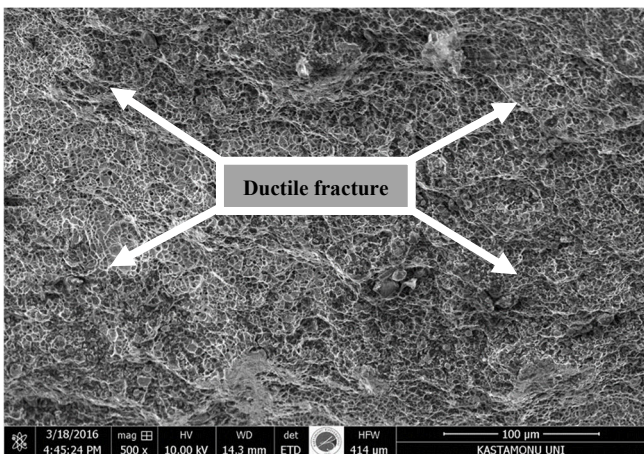
Figure 15. Fracture surface image of Experiment 7
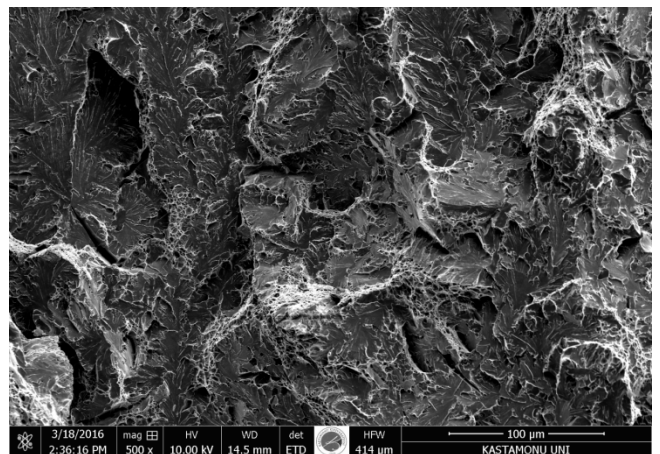
Figure 18. Fracture surface image of Experiment 10
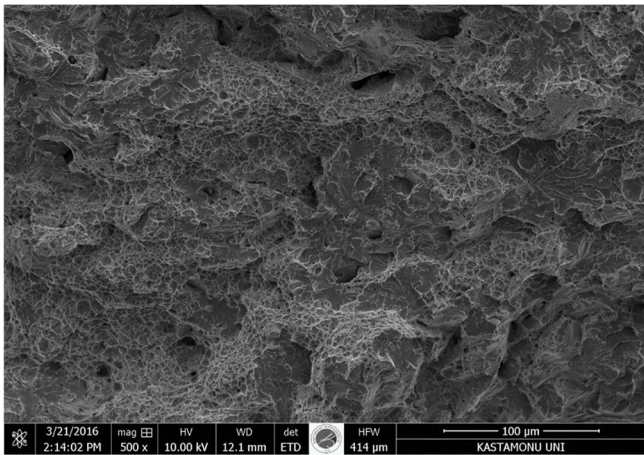
Figure 19. Fracture surface image of Experiment 11
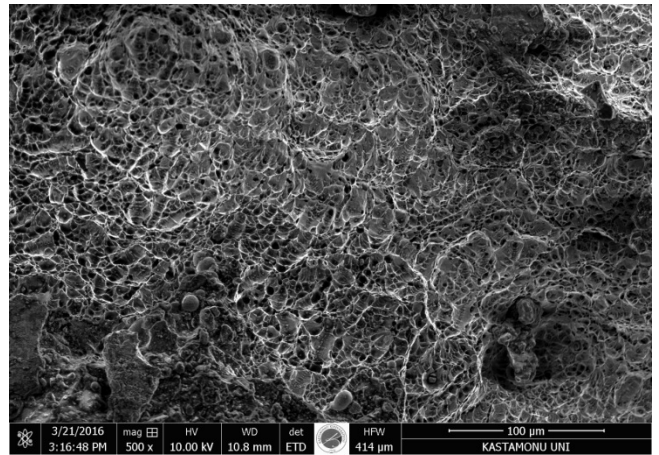
Figure 23. Fracture surface image of Experiment 15
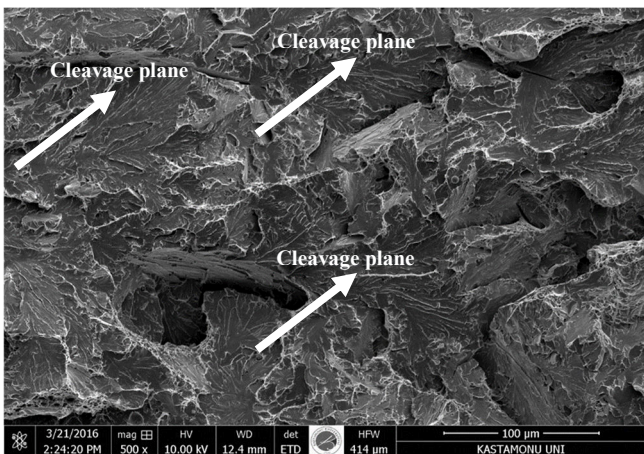
Figure 20. Fracture surface image of Experiment 12
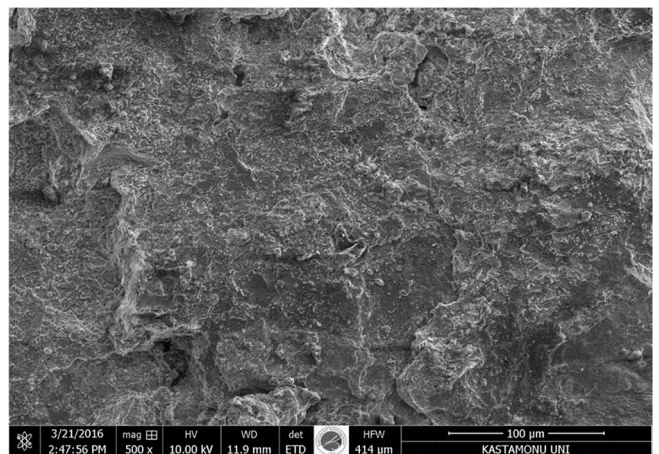
Figure 24. Fracture surface image of Experiment 16
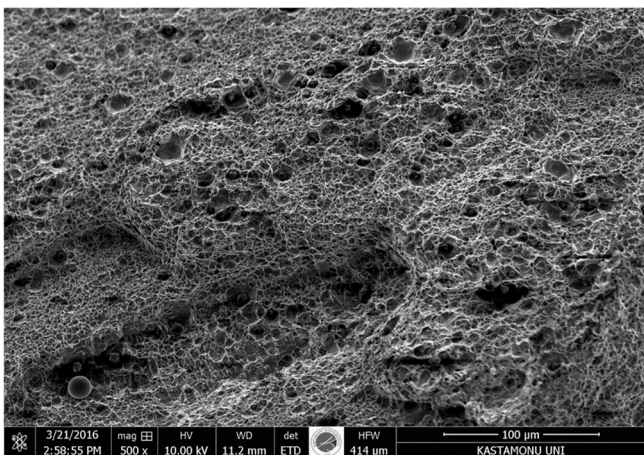
Figure 21. Fracture surface image of Experiment 13

When SEM images of the fracture surfaces were examined, the elongations and orientations exhibited by the grains indicated that there were generally ductile fractures in all of the joints that were welded from bottom to top. Since the fractures occurred both inside the grain and at the grain boundary in the joints (1, 3, 5, 7, 9, 11, 13 and 15 joints) welded from bottom to top, fracture elongations took place on the entire surface of the material, therefore fracture surface exhibited a ductile behavior. The breakage of the aforementioned samples generally occurred as a result of sliding fracture. In addition, fractures were generally ductile as they occurred with the effect of plastic deformation. In a study, İrfan Ay [13] stated that dislocation movements had terminated at remains and grain boundaries, and in these regions, firstly cavities had formed, then these cavities had expanded by merging and fracture surfaces had formed in a matt and fibrous structure. It is thought from the fractures occurring in a single piece, fibrous structures and equiaxed honeycomb like views that fractures occurred by exhibiting a ductile behavior. Fractures of the aforementioned joints having is seen as a natural result since the heat input is high in the upward direction.ductile and honeycomb like structure. In

Figure 22. Fracture surface image of Experiment 14

addition, bridges were formed between voids when they got large enough and a honeycomb appearance occurred. Therefore, it is possible to see a honeycomb like appearance along with a fibrous structure in the images.

Although in the joints (2, 4, 6, 8, 10, 12, 14, 16) that were welded from top to bottom, although fibrous structures that exhibited ductile behavior from place to place were seen in the images, it was observed that the fractures generally exhibited a brittle behavior and occurred on cleavage planes. Joints from top to bottom are joints that are less of heat input and cooling time due to welding direction. As the heat input is less at these junctions, cleavage planes were formed along with fibrous and fibrous structures in the main matrix. This points to brittle fracture.

From the above expressions, it is possible to say that fracture behavior varies depending on the welding direction. Excessive heating and slow cooling in the upward direction, which naturally has a more intense heat input, allowed formation of coarser grained structures in these joins, resulting in a more ductile fracture of the materials in the nick break tests. On the other hand in the welded joints made in downward direction, since the heat input was less, the joints were down faster and relatively fine-grained structures were formed. This revealed, in the fracture surface images obtained from the welded joints, the presence of cleavage planes indicating brittle fracture along with fibrous structures indicating ductile fracture. The microstructure of API 5L X65 pipe steel used in the experiments consists of as low pearlitic, ferritic matrix. Size of the microstructure, perlite volume ratio and microalloy element ratio have an effect on fracture behavior. As ferrite volume ratio increase, properties of fracture mechanics improve. X65 steel has superior properties in terms of both small grain size and high ferrite volume ratio. The most effective method for toughness, strength and weldability is to reduce grain size. The increase in the toughness of a fine grained structure is explained by the increase of the flow limit; as grain size is reduced, onset of plastic deformation is put off to higher stresses. For this reason, in the breakages of the samples, onset of deformation was put off to higher stresses and properties of fracture mechanics were improved [14-16].

Generally; ductile, semi ductile and brittle fracture modes were seen on SEM images of API 5L X65 steel pipe joints. Similar studies support these determinations. Kingklang and Uthaisangsuk reported that the API 5L X65 steel has a ductile fracture structure [17]. Liu et al. reported that the cavities were formed on the fracture surfaces of the X70 steel together with ductile fracture [18]. In another study, Maruschak et al. examined the fracture mechanics of various pipelines and reported both types of fracture were observed in their surface studies [19]. Also Yonghe et al. reported that the API 5L X80 steel exhibits a ductile fracture with deep cavities and have a good plastic deformation properties [20].

5. CONCLUSION

- API 5L pipe steels, which were prepared in accordance with the API 1104 standard, were welded with different electrodes and in different directions. They were subjected to nick break tests and the following results were obtained from macro and sem images of the fracture surfaces of the samples; when the nick break test results were examined, within the scope of visual inspection, all welded joints were accepted except experiments 2 and 4. In experiments 2 and 4, lack of fusion or inadequate penetration was observed. The radiographic and macrographic examinations of the aforesaid samples also confirmed this result.
- When SEM images of the fracture surfaces were examined, the elongations and orientations exhibited by the grains indicated that there were generally ductile fractures in all of the joints that were welded from bottom to top. In the joints that were welded from top to bottom, on the other hand, although fibrous structures indicating ductile fracture were seen in places in the images together with cleavage planes indicating brittle fracture were observed.
- It was understood from the images formed by the equiaxed honeycomb like and fibrous structures in SEM analyses revealed that the fractures of the joints that were welded in the upward direction generally exhibited a ductile behavior and the fact that fractures occurred in a single piece again indicated a ductile breakage.
- Excessive heating and slow cooling in the upward direction, which has a more intense heat input due to its welding position, allowed formation of coarser grained structures in these

joins, resulting in a more ductile fracture of the materials in the nick break tests

• In the joints welded in downward direction, on the other hand, the heat input was less, the joints were heated less, cooled down faster and relatively fine-grained structures were formed, when compared to the experiments conducted in upward direction. This revealed, in the fracture surface images obtained from the welded joints, the presence of cleavage planes indicating brittle fracture along with fibrous structures indicating ductile fracture. In the joints welded in downward direction, both ductile and brittle fracture types were observed.

6. ACKNOWLEDGEMENT

REFERENCES

[1] F. Umbach,"Global energy security and the implications for the EU," *Energy Policy*, 38, 1229–1240, 2010.

[2] H. Ada, S. Aksöz, T. Fındık, C. Çetinkaya, and M. Gülsün, "Tozaltı kaynak yöntemiyle birleştirilen petrol ve doğalgaz borularının mikroyapı ve mekanik özelliklerinin incelenmesi," *Politeknik Dergisi,* 19 (3), 275-282, 2016.

[3] H. Ada, S. Aksöz, T. Fındık, C. Çetinkaya, B. Bostan and İ. Candan, "API 5L X65 Çeliklerinin MAG Kaynak Yöntemi ile Birleştirilmesinde, Kaynak İşleminin Mikroyapı ve Mekanik Özelliklere Etkisinin İncelenmesi," *Çukurova University Journal of the Faculty of Engineering and Architecture*, 31, (ÖS 1), 1- 9, 2016.

[4] API Specifications 5L, "Specifications for Line Pipe". 45th Edition, *American Petroleum Institute*, USA, 2012.

[5] S.H. Hashemi, "Strength - hardness statistical correlation in API X65 steel," *Mater. Sci. Eng. A*, 528, 1648–1655, 2011.

[6] M. Rakhshkhorshid, S.H. Hashemi, "Experimental study of hot deformation behavior in API X65 steel," *Materials Science & Engineering A*, 573, 37–44, 2013.

[7] S.H. Hashemi, D. Mohammadyani, "Characterization of weldment hardness, impact energy and microstructure in API X65 steel," *Int. J. Pressure Vessels Piping*, 98, 8–15, 2012.

[8] A. Radovic, N. Bajic, and V. Grabulov, "Specific quality of the weld metal of welded joints of finegrained microalloyed steels," *Zavarivanje* 96, 61–72, 1996.

[9] N. Bajic, V. Sijacki-Zeravcic, M. Rakin, and K. Kovacevic, "Structure optimization of weld metal and HAZ in microalloyed high strength steel welded joints," *Yucomat, Herceg Novi*, 193–200, 2005.

[10] Bajic and, N.V. Šijaki-Žeravi, "The analysis of change of structural and mechanical properties of welded joints of microalloyed Nb/V steel grade by changing the composition of filler material," *Internat. Conf. On Welding,* Belgrade, 2003.

[11] B.E. Rani Amitha, and J. Bharathibai Basu, "Green corrosion inhibitors - an overview," *Technical Report, National Aerospace Laboratories*, Bangalore, India, 2009.

[12] M.A. Migahed, A.M. Al-Sabagh, E.A. Khamis, E.G. Zaki, "Quantum Chemical calculations, synthesis and corrosion inhibition efficiency of ethoxylated- [2- (2 - {2 - [2- (2 –benzen esulfonylaminoethylamino) - ethylamino] - ethylamino} - ethylamino) - ethyl] -4 - alkyl benzenesulfonamide on API X65 steel surface under H2S environment," *Journal of Molecular Liquids*, 212, 360–371, 2015.

[13] http://w3.balikesir.edu.tr/~ay/lectures/km/lecture1.pdf

[14] K.E. Hagedorn, R. Kaspar, and R. Kleine, "Untersuchungen zum einfluss des gefügesauf bruchmechanische kennwerte," *Steel Research*, 61(10), 510-517, 1990.

[15] Z. Taş, "Termomekanik İşlem Görmüş Mikroalaşımlı Çeliklerin Kırılma Mekaniği - Kırılma Tokluğu- Açısından İncelenmesi, *Doktora Tezi"* YTÜ Fen Bilimleri Enstitüsü, İstanbul, 107, 2004.

[16] Tang J., Liu Z., Shi S, Chen X, "Evaluation of fracture toughness in different regions of weld joints using unloading compliance and normalization method", *Engineering Fracture Mechanics,* 195: 1–12, 2018.

[17] Kingklang S., Uthaisangsuk V, "Plastic deformation and fracture behavior of X65 pipeline steel: Experiments and modeling", *Engineering Fracture Mechanics*, 191:82-101, 2018.

[18] Liu L., Xiao H., Li Q., Liu Y., Li P., Yang Z., Yu H, "Evaluation of the fracture toughness of X70 pipeline steel with ferritebainite microstructure", *Materials Science & Engineering A,* 688:388–395, 2017.

[19] Maruschak P.O., Panin S.V.,. Chausov M.G., Bishchak R.T., Polyvana U.V, "Effect of long-term operation on steels of main gas pipeline. Reduction of static fracture toughness", *Journal of Natural Gas Science and Engineering,* 38:182-186, 2017.

[20] Yonghe Y., Lei S. Zhen X. Hongsheng L., Xu C., Xin W., "Fracture toughness of the materials in welded joint of X80 pipeline steel", *Engineering Fracture Mechanics,* 148:337–349, 2015.

[21] Yang Z., "The Fracture during Drop-Weight Tear Test of High Performance Pipeline Steel and Its Abnormal Fracture Appearance", *Procedia Materials Science*, 3:1591–1598, 2014.